J|A|C|S ARTICLES

Published on Web 01/06/2009

Detecting Protein–Ligand Binding on Supported Bilayers by Local pH Modulation

Hyunsook Jung, Aaron D. Robison, and Paul S. Cremer*

Department of Chemistry, Texas A&M University, P.O. Box 30012, College Station, Texas 77843-3012

Received June 14, 2008; E-mail: cremer@mail.chem.tamu.edu

Abstract: Herein, we describe a highly sensitive technique for detecting protein–ligand binding at the liquid/solid interface. The method is based upon modulation of the interfacial pH when the protein binds. This change is detected by *ortho*-Texas Red DHPE, which is doped into supported phospholipid bilayers and used as a pH-sensitive dye. The dye molecule fluoresces strongly at acidic pH values but not basic ones and has an apparent pK_A of 7.8 in 1-palmitoyl-2-oleoyl-*sn*-glycero-3-phosphocholine membranes containing 0.5 mol % biotin-cap-PE. This method was used to detect antibiotin/biotin binding interactions as well as the binding of cholera toxin B subunits to GM_1. Since these proteins are negatively charged under the conditions of the experiment the interface became slightly more acidic upon binding. In each case, the equilibrium dissociation constant was determined by following the rise in fluorescence as protein was introduced. This change is essentially linear with protein coverage under the conditions employed. For the biotin/antibiotin system it was determined that $K_D = 24 \pm 5$ nM, which is in excellent agreement with classical measurements made by total internal reflection fluorescence microscopy involving fluorophore-conjugated antibody molecules. Moreover, the limit of detection was ~350 fM at the 99% confidence level. This corresponds to 1 part in 69 000 of the K_D value. Such a finding compares favorably with surface plasmon resonance studies of similar systems and conditions. The assay could be run in imaging mode to obtain multiple simultaneous measurements using a CCD camera.

Introduction

Ligand–receptor binding is ubiquitous in the chemical and biological sciences. Monitoring such interactions is often performed by fluorescently labeling the proteins or nucleotides of interest. In fact, fluorescent tags have become a standard tool for detecting biomolecules. Protein labeling can, however, interfere with detection measurements and be highly inconvenient to employ.[1] This has been a major driving force behind the development of assays that can detect biological analytes in a label-free fashion. To date, methods include the use of liquid crystalline phase transitions,[2,3] colloidal particle phase transitions,[4] nanoparticles,[5−7] semiconductor nanowire conductivity,[8−10] quartz crystal microbalance (QCM) measurements,[11−13] and surface plasmon resonance (SPR) spectroscopy[14]/imaging (SPRI).[15−17] Most of these techniques are performed at interfaces, but techniques to detect analytes in bulk solution are also being developed.[18,19]

Despite the tremendous progress in label-free detection, no technique to date offers the sensitivity and flexibility of fluorescence-based measurements. Indeed, fluorescence measurements can routinely be made down to the single molecule level without the need for subsequent signal amplification steps. Moreover, fluorescent-based devices provide rapid readout and can be easily employed in an array-based format. Finally, with the exception of the protein tagging step itself, fluorescence spectroscopy/microscopy is relatively easy to perform. These

(1) Tan, P. K.; Downey, T. J.; Spitznagel, E. L.; Xu, P.; Fu, D.; Dimitrov, D. S.; Lempicki, R. A.; Raaka, B. M.; Cam, M. C. *Nucleic Acids Res.* **2003**, *31*, 5676–5684.
(2) Kim, S. R.; Abbott, N. L. *Adv. Mater.* **2001**, *13*, 1445–1449.
(3) Brake, J. M.; Daschner, M. K.; Luk, Y. Y.; Abbott, N. L. *Science* **2003**, *302*, 2094–2097.
(4) Baksh, M. M.; Jaros, M.; Groves, J. T. *Nature* **2004**, *427*, 139–141.
(5) Nam, J. M.; Stoeva, S. I.; Mirkin, C. A. *J. Am. Chem. Soc.* **2004**, *126*, 5932–5933.
(6) Nam, J. M.; Thaxton, C. S.; Mirkin, C. A. *Science* **2003**, *301*, 1884–1886.
(7) Stoeva, S. I.; Lee, J. S.; Smith, J. E.; Rosen, S. T.; Mirkin, C. A. *J. Am. Chem. Soc.* **2006**, *128*, 8378–8379.
(8) Cui, Y.; Wei, Q. Q.; Park, H. K.; Lieber, C. M. *Science* **2001**, *293*, 1289–1292.
(9) Patolsky, F.; Zheng, G. F.; Lieber, C. M. *Anal. Chem.* **2006**, *78*, 4260–4269.
(10) Wang, W. U.; Chen, C.; Lin, K. H.; Fang, Y.; Lieber, C. M. *Proc. Natl. Acad. Sci. U.S.A.* **2005**, *102*, 3208–3212.
(11) Muratsugu, M.; Ohta, F.; Miya, Y.; Hosokawa, T.; Kurosawa, S.; Kamo, N.; Ikeda, H. *Anal. Chem.* **1993**, *65*, 2933–2937.
(12) Cooper, M. A.; Dultsev, F. N.; Minson, T.; Ostanin, V. P.; Abell, C.; Klenerman, D. *Nat. Biotechnol.* **2001**, *19*, 833–837.
(13) Yao, C. Y.; Chen, Q. H.; Chen, M.; Zhang, B.; Luo, Y.; Huang, Q.; Huang, J. F.; Fu, W. L. *J. Nanosci. Nanotechnol.* **2006**, *6*, 3828–3834.
(14) Yang, C. Y.; Brooks, E.; Li, Y.; Denny, P.; Ho, C. M.; Qi, F. X.; Shi, W. Y.; Wolinsky, L.; Wu, B.; Wong, D. T. W.; Montemagno, C. D. *Lab on a Chip* **2005**, *5*, 1017–1023.
(15) Brockman, J. M.; Frutos, A. G.; Corn, R. M. *J. Am. Chem. Soc.* **1999**, *121*, 8044–8051.
(16) Wegner, G. J.; Lee, H. J.; Corn, R. M. *Anal. Chem.* **2002**, *74*, 5161–5168.
(17) Lee, H. J.; Nedelkov, D.; Corn, R. M. *Anal. Chem.* **2006**, *78*, 6504–6510.
(18) Markov, D. A.; Swinney, K.; Bornhop, D. J. *J. Am. Chem. Soc.* **2004**, *126*, 16659–16664.
(19) Bornhop, D. J.; Latham, J. C.; Kussrow, A.; Markov, D. A.; Jones, R. D.; Sørensen, H. S. *Science* **2007**, *317*, 1732–1736.

 10.1021/ja804542p CCC: $40.75

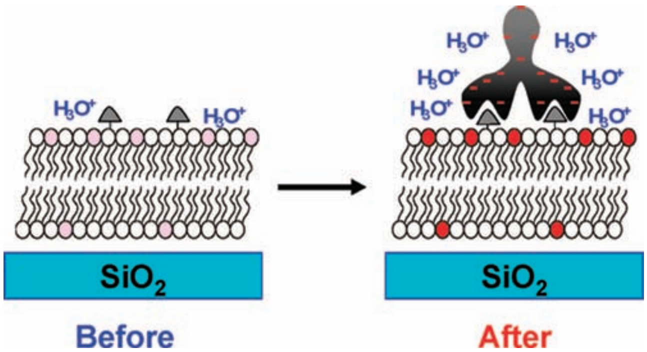

Figure 1. Schematic diagram illustrating the principle of a pH-sensitive dye as a reporter for interfacial binding of negatively charged proteins. (Before) In the absence of proteins, the dye molecules fluoresce relatively weakly. (After) Upon specific protein binding, the dye molecules fluoresce strongly.

advantages raise the question as to whether such techniques could be exploited for interfacial analyte detection without the need for tagging the target molecule. Instead, a fluorescent dye would be embedded onto the surface of a detection platform and employed as a universal sensing element for ligand/receptor binding in much the same way that fluorescent dyes can be used to sense changes in pH or metal ion concentrations in bulk solution. Surprisingly, relatively little work has been performed until now to explore the use of fluorophores as an integral part of sensor platforms for detecting biomacromolecule binding. In one example, Swanson and co-workers exploited the aggregation of ligand-conjugated dye molecules to detect multivalent protein binding via a fluorescence quenching mechanism.[20,21] Also, Groves and co-workers exploited the change in the diffusion of membrane-bound fluorophores to detect protein binding.[22]

Herein, we employ pH-sensitive fluorescent dye molecules to create biosensors that can be employed to monitor multivalent ligand−receptor interactions on supported lipid bilayers (SLBs). The dye fluoresces strongly in the protonated state but becomes inactive upon deprotonation. The underlying physical principle for our detection method is based upon the idea that the binding of proteins to ligands at a surface will perturb the interfacial pH relative to the bulk value. Most proteins are negatively charged at physiological pH. Therefore, when these biomacromolecules adsorb on a surface they recruit hydronium ions with them and thereby lower the interfacial pH. Such local acidification is then reported by membrane-bound fluorophores near their titration point. A schematic diagram of this concept is shown in Figure 1. As can be seen, ligands (gray triangles) are incorporated into an SLB along with pH-sensitive fluorescent dye molecules (shown in pink). The fluorophores are initially inactive. The binding of the negatively charged protein causes them to protonate and fluoresce strongly (shown in red). Precedence for this interfacial sensing idea is based upon the nonspecific adsorption of charged polymers to oppositely charged surfaces to change the surface potential. For example, the pH-sensitive fluorophore hydroxycoumarin has been employed to monitor the loading of DNA onto cationic liposomes in aqueous solution.[23,24] Moreover, it has been suggested that this concept might be applicable for other types of biomolecules, although no experiments were attempted.[25]

Most proteins possess a relatively modest charge per unit mass near physiological pH compared with DNA. Therefore, one needs to employ a very stable fluorophore as the pH-sensitive interfacial detection element. Moreover, a suitable control system against which pH changes can be measured is also required. Texas Red DHPE is an ideal candidate for such measurements (Figure 2). Texas Red DHPE is made from Texas Red sulfonyl chloride via addition of the free amine from the headgroup of 1,2-dihexadecanoyl-*sn*-glycero-3-phosphoethanolamine (DHPE). Because Texas Red sulfonyl chloride consists of an ortho and a para isomer,[26] the conjugated lipid product is ultimately an isomeric mixture. The ortho-conjugated isomer fluoresces when the sulfonamide is protonated but not when it is deprotonated (Figure 2a).[27] The process is perfectly reversible, and it is possible to toggle back and forth between the two states by raising and lowering the pH.[26] This isomer is suitable for use as a pH sensor. By contrast, the para isomer of Texas Red DHPE is a pH-insensitive dye and can be employed as a reference for determining relative changes in fluorescence intensity of the ortho-conjugated dye (Figure 2b). It should be noted that it is straightforward to separate the ortho and para isomers via thin layer chromatography (TLC) as well as by electrophoretic separation in a bilayer matrix.[28]

Herein, we demonstrate the use of ortho-conjugated Texas Red DHPE as a reporter of local pH modulation in supported lipid bilayers. The apparent pK_A of this molecule in an SLB containing 0.5 mol % biotin-cap-PE on glass was found to be 7.8 ± 0.1. The dye molecule could be used to generate a binding curve for the biotin/antibiotin pair at the SLB interface. The equilibrium dissociation constant, K_D, was found to be 24 ± 5 nM. This value is in good agreement with measurements made by total internal reflection fluorescence microscopy (TIRFM) using dye-labeled proteins. Moreover, the limit of detection (LOD) for the antibody was ~350 fM at the 99% confidence level. This is about 69 000 times smaller than the corresponding K_D value. In imaging mode, the assay could detect fewer than 400 IgG molecules in a single 4×4 binned pixel region. Thus, this assay compares extremely favorably with previously developed detection techniques.

Experimental Section

Materials. Texas Red DHPE was purchased from Invitrogen (Eugene, OR). Rabbit polyclonal antibiotin antibody came from Rockland (Gilbertsville, PA), while affinity purified goat polyclonal antidinitrophenyl (anti-DNP) IgG was obtained from Axxora (San Diego, CA). Cholera toxin B from *Vibrio cholerae* was purchased from Sigma-Aldrich (St. Louis, MO). POPC (1-palmitoyl-2-oleoyl-*sn*-glycero-3-phosphocholine), biotin-cap-PE (1,2-dipalmitoyl-*sn*-glycero-3-phosphoethanolamine-*N*-(cap biotinyl) (sodium salt), DOPC (1,2-dioleoyl-*sn*-glycero-3-phosphocholine), DPPC (1,2-

(20) Song, X. D.; Nolan, J.; Swanson, B. I. *J. Am. Chem. Soc.* **1998**, *120*, 4873–4874.
(21) Song, X. D.; Nolan, J.; Swanson, B. I. *J. Am. Chem. Soc.* **1998**, *120*, 11514–11515.
(22) Yamazaki, V.; Sirenko, O.; Schafer, R. J.; Groves, J. T. *J. Am. Chem. Soc.* **2005**, *127*, 2826–2827.
(23) Zuidam, N. J.; Barenholz, Y. *Biochim. Biophys. Acta* **1998**, *1368*, 115–128.
(24) Zuidam, N. J.; Barenholz, Y. *Biochim. Biophys. Acta* **1997**, *1329*, 211–222.
(25) Barenholtz, Y.; Hirsch-Lerner, D.; Cohen, R.; Dagan, A.; Gatt, S. U.S. Patent 7056653 B2, 2006.
(26) Corrie, J. E. T.; Davis, C. T.; Eccleston, J. F. *Bioconjugate Chem.* **2001**, *12*, 186–194.
(27) Marchesini, S.; Gatt, S.; Agmon, V.; Giudici, M. L.; Monti, E. *Biochem. Int.* **1992**, *27*, 545–550.
(28) Daniel, S.; Diaz, A. J.; Martinez, K. M.; Bench, B. J.; Albertorio, F.; Cremer, P. S. *J. Am. Chem. Soc.* **2007**, *129*, 8072–8073.

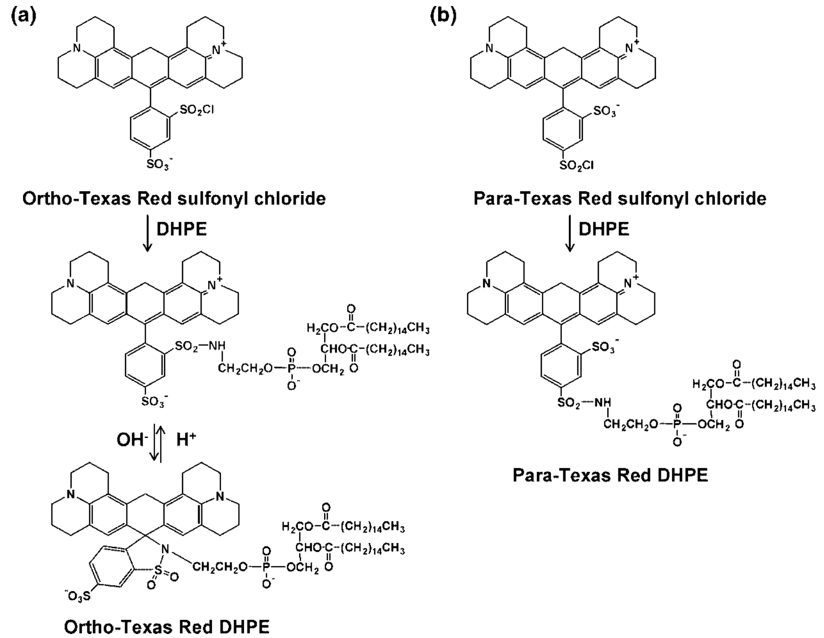

Figure 2. (a) Ortho and (b) para forms of Texas Red sulfonyl chloride are shown at the top. Both isomers can be conjugated to a primary amine (DHPE in this case). The ortho isomer forms a five-membered ring upon deprotonation of the sulfonamide by attacking the xanthylium ring system (a). The para isomer does not undergo an equivalent reaction because of geometric constraints (b).

dipalmitoyl-*sn*-glycero-3-phosphocholine), ganglioside GM_1 (brain, ovine-ammonium salt), and cholesterol were obtained from Avanti Polar Lipids (Alabaster, AL). Thin layer chromatography (TLC) was carried out using precoated plates made of silica gel with a pore size of 60 Å and a layer thickness of 250 μm (Silica Gel 60 F_{254}, EMD Chemicals Inc., Germany). Purified water was produced from a NANOpure Ultrapure Water System (18.2 MΩ·cm, Barnstead, Dubuque, IA). Glass coverslips (25 × 25 mm, No. 2, Corning Inc.) were used as solid supports for the bilayers. Polydimethylsiloxane (PDMS, Dow Corning Sylgard Silicone Elastomer-184) was obtained from Krayden, Inc. (El Paso, TX).

Separation of Texas Red DHPE Isomers. The two isomers of Texas Red DHPE were separated using a slightly modified form of our previously published procedures.[28] Briefly, small spots of the ortho/para mixture were made on a TLC plate from a 1 mg/mL chloroform solution. Next, the spotted plate was placed into a development chamber, and ethanol (AAPER Alcohol and Chemical Co., Shelbyville, KY) was used as the eluent. Two bands were formed, whereby the upper band was the para isomer and the lower band was the ortho isomer. Each band was recovered separately from the plate by carefully scraping the surface with a razor blade and resuspending the dye/silica bead mixture in methanol. The silica was separated from the soluble organic material by filtration. Methanol could then be removed using a rotary pump and further drying the sample under vacuum on a Schlenk line. TLC was rerun with a small portion of the isolated sample to confirm the purity of each isomer.

Preparation of Small Unilamellar Vesicles (SUVs). Lipids in the desired composition ratio were introduced into a glass vial in chloroform. The solvent was removed by passing a gentle stream of dry nitrogen over the solution. The resulting film was further dried under vacuum for 3 h. The film was then hydrated in a 10 mM phosphate-buffered saline (PBS) solution containing 150 mM NaCl. After suspension of the lipid mixture it was subjected to 10 freeze−thaw cycles and then extruded 10 times through two stacked polycarbonate membranes (Whatman) with 100 nm pores. The resulting SUVs prepared by this procedure were 70 ± 10 nm in diameter as determined by dynamic light scattering (Brookhaven Instruments 90Plus Particle Size Analyzer). The final concentration of the lipid solutions employed for vesicle fusion experiments was 0.5 mg/mL. The vesicles were kept at 4 °C before use.

pH Titration and Buffer Preparation. Ten millimolar PBS solutions containing 150 mM NaCl were prepared at pH values ranging from 4.0 to 10.2 by mixing appropriate amounts of Na_2HPO_4, NaH_2PO_4, or Na_3PO_4. These pH values were chosen to locate the pK_A value of *ortho*-Texas Red DHPE. The pH could be adjusted to the desired value by dropwise addition of HCl or NaOH. The pH was measured with a standard glass electrode setup. Such absolute measurements had an error of ±0.1 pH units associated with them. Changes in fluorescence, however, could be measured far more accurately. These changes in fluorescence intensity corresponded to relative shifts in interfacial pH as small as 0.002 pH units when a 40× objective was employed for making the measurements. Titration curves for the dye molecules in SLBs were obtained by systematically changing the pH of the bulk solution in a stepwise fashion. Fresh buffer was continuously flowed over the surface until no further changes in fluorescence intensity could be observed. The quality and fluidity of the supported bilayers as a function of pH was confirmed by fluorescence recovery after photobleaching (FRAP) measurements.[29] These results are provided in the Supporting Information (Figures S1 and S2). Fluorescent micrographs of SLBs were captured with a standard epifluorescence microscope setup (Nikon Eclipse E800).

The fluorescence titration curve of the Texas Red DHPE dye molecules was monitored in SLBs containing two narrow, parallel lines of bilayers with distinct dye chemistries. The first line contained 99.47 mol % POPC/0.50 mol % biotin-cap-PE/∼0.03 mol % *ortho*-Texas Red DHPE. The second line was identical but contained *para*-Texas Red DHPE instead of the ortho isomer. The surrounding lipid matrix was a 1:1:1 mixture of DOPC, DPPC, and cholesterol. This composition was chosen because diffusion of the dye molecules from the narrow lines into the surrounding matrix was extremely slow. The two lines were formed sequentially by mechanically scratching the DOPC/DPPC/cholesterol bilayer and backfilling with the desired lipid mixture using the vesicle fusion method.[30]

The titration curve for the Texas Red DHPE dye molecules in the presence of a saturated antibiotin protein monolayer on a

(29) Diaz, A. J.; Albertorio, F.; Daniel, S.; Cremer, P. S. *Langmuir* **2008**, *24*, 6820–6826.
(30) Mao, H.; Yang, T.; Cremer, P. S. *Anal. Chem.* **2002**, *74*, 379–385.

supported membrane surface was obtained with the same bilayer as described above. In this case, however, a saturation concentration of IgG (500 nM) was first introduced into the bulk solution. Moreover, all fluorescence measurements as a function of pH were performed in the presence of 500 nM bulk protein concentration to ensure that the surface remained saturated with protein.

All experiments presented herein were conducted with 150 mM NaCl. Additional control experiments were performed with varying concentrations of salts up to 300 mM. The results showed that fluorescence changes upon protein binding were not affected within experimental errors when moderately high salt concentrations were present. This is to be expected because the Debye length is below 1 nm so long as there is at least 100 mM NaCl in the buffer solution.[31]

Fabrication of Microfluidic Devices. Seven-channel microfluidic devices (130 μm wide, 15 μm deep, and separated by 160 μm spacing) were formed by conventional soft lithographic methods.[32] First, glass substrates (soda-lime glass slides, Corning) were spin coated with photoresist (Shipley 1827) and then exposed to UV light through a Kodak technical pan film photomask containing the appropriate image. After the substrates were treated in developing solution and baked overnight at 120 °C, they were immersed in a buffered oxide echant (BOE) to etch the glass. The BOE solution was prepared with a 1:6 ratio (v/v) of 48% HF (EMD Chemicals Inc., Germany) and aqueous NH_4F (200 g in 300 mL purified water, Alfa Aesar, Ward Hill, MA).[33] The remaining photoresist was removed with acetone. Next, a degassed mixture of Sylgard silicone elastomer-184 and a curing agent (10:1 ratio (v/v)) was poured over the patterned glass substrate. The liquid PDMS was cured in an oven at 70 °C for 1 h and then peeled off the glass substrate. This elastomeric mold and a freshly cleaned glass coverslip were placed into a 25 W oxygen plasma for 30 s and immediately brought into contact to form the PDMS/glass device. The glass slides used in these experiments were cleaned in a boiling solution of ICN 7X (Costa Mesa, CA) and purified water (1:4 ratio (v/v)) for 30 min, rinsed with copious amounts of purified water, and dried gently under a flow of nitrogen gas. Finally, the glass substrates were annealed in a kiln at 450 °C for 5 h before introduction into the oxygen plasma.

Formation of Supported Bilayers. SLBs were formed on the walls and floors of microchannels by spontaneous fusion of SUVs.[34] To do this, 5 μL of an SUV solution was injected into each channel immediately after formation of a PDMS/glass device. The solutions were incubated in the channels for 10 min and then rinsed away with pure PBS buffer (pH 8.2) to remove excess vesicles.

To make binding constant measurements, varying concentrations of unlabeled antibody solutions were continually injected into each microchannel at a rate of 200 nL/min until the fluorescence intensity from the surface remained constant. This took up to ~5 h for the lowest protein concentration measurements.

Epifluorescence Microscopy. An inverted epifluorescence Nikon Eclipse TE2000-U microscope with a 10× air objective (N.A. = 0.45) was used for FRAP studies. Laser radiation from a 2.5 W mixed gas Ar^+/K^+ laser (Stabilite 2018, Spectra Physics) was used to bleach a small spot (14 μm in diameter) in the supported bilayer sample.

Fluorescence imaging studies were performed with a Nikon Eclipse E800 fluorescence microscope (Tokyo, Japan) equipped with a MicroMax 1024 CCD camera (Princeton Instruments), a Texas Red filter set (Chroma Technology, Bellows Falls, VT), and either a 4× air (N.A. = 0.13) or a 10× air (N.A. = 0.45) objective.

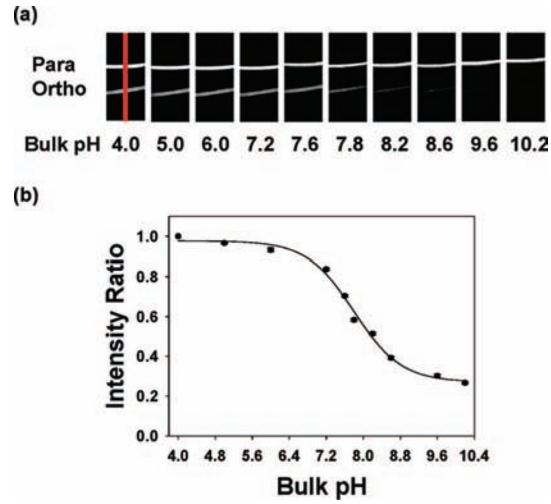

Figure 3. (a) Fluorescence images of supported POPC bilayers containing para- and ortho-conjugated Texas Red DHPE in two adjacent bands. Each bilayer strip contained 0.5 mol % biotin-cap-PE and ~0.03 mol % of the respective fluorescent dye. The images were taken from pH 10.2 to 4.0. A 4× air objective was used to make these measurements. An example of the region from which intensity line profile data was abstracted is denoted with a red line in the first image. (b) Relative intensity for the ortho-conjugated isomer of Texas Red DHPE as a function of pH. The black circles represent individual fluorescence measurements, and the solid line is a sigmoidal fit to the data. Error bars representing standard deviation measurements from three data sets are denoted on each data point. To obtain the *y* axis, the intensity of the ortho band was divided by the intensity of the para band at each pH value. This ratio was normalized to 1.0 at pH 4.0. All intensity ratios are relative to this normalization.

An X-Cite 120 arc lamp (EXFO) was used as the light source for all experiments, and all images were processed with MetaMorph software (Universal Imaging). Data acquisition for the limit of detection experiments was also performed in epifluorescence mode. In this case, a 40× oil immersion objective (N.A. = 1.30) was used to monitor the fluorescence intensity.

Classical Binding Measurements. Binding measurements with labeled antibodies were performed inside microfluidic devices which were identical to those described above. Protein detection was done with total internal reflection fluorescence microscopy (TIRFM).[34,35] Alexa Fluor-594 tags were conjugated to the antibiotin molecules using an Invitrogen labeling kit (Eugene, OR) by following standard procedures. The labeled antibody solutions at various concentrations (PBS buffer, pH 8.2) were flowed through each microchannel until the bulk fluorescence intensity from the dye-labeled antibodies remained constant as judged by epifluorescence measurements. A 594 nm helium–neon laser beam (4 mW, Uniphase, Manteca, CA) was projected onto the sample with a line generator lens (BK7 for 30°, Edmund Optics, Barrington, NJ) for TIRFM measurements. This created a uniform intensity profile perpendicular to the direction of flow of the microfluidic channels. On the other hand, the intensity of the beam parallel to the long axis of the channels corresponded to a Gaussian profile. The glass substrates for the microfluidic devices were optically coupled to a dove prism with index matching immersion oil (type DF, Cargille Laboratories, Ceder Grove, NJ).

Results

Titration Curves for *ortho*-Texas Red DHPE. In a first set of experiments the pH-dependent responses of the ortho- and para-conjugated Texas Red dyes were investigated in supported POPC bilayers with 0.5 mol % biotin-cap-PE. Titration experi-

(31) Israelachivili, J. N. *Intermolecular and Surface Forces*, 2nd ed.; Academic Press: San Diego, CA, 1991.
(32) Shi, J. J.; Yang, T.; Kataoka, S.; Zhang, Y.; Diaz, A. J.; Cremer, P. S. *J. Am. Chem. Soc.* **2007**, *129*, 5954–5961.
(33) Holden, M. A.; Kumar, S.; Castellana, E. T.; Beskok, A.; Cremer, P. S. *Sensors Actuators B* **2003**, *92*, 199–207.
(34) Jung, H. S.; Yang, T.; Lasagna, M. D.; Shi, J. J.; Reinhart, G. D.; Cremer, P. S. *Biophys. J.* **2008**, *94*, 3094–3103.
(35) Yang, T.; Baryshnikova, O. K.; Mao, H.; Holden, M. A.; Cremer, P. S. *J. Am. Chem. Soc.* **2003**, *125*, 4779–4784.

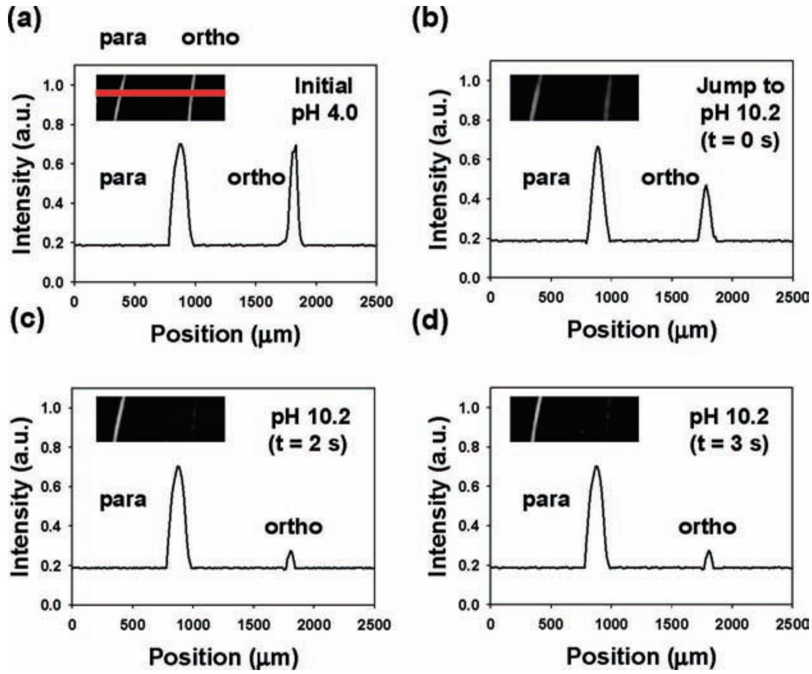

Figure 4. Time response of ortho- and para-conjugated Texas Red DHPE bands in a supported bilayer to an abrupt jump in pH from 4.0 to 10.2: (a) pH originally set to 4.0; (b) buffer solution at pH 10.2 is flowed over the surface, (c) 2 s later, and (d) 3 s later. Both an epifluorescence image and a corresponding line profile are shown for each time period. An example of the region across which the line profile was taken is denoted with a red line in (a). A 4× air objective was used to make these measurements.

ments were systematically performed by changing the pH of the bulk solution stepwise from pH 10.2 to 4.0. Bulk solutions at a given pH were continuously flowed into the device until the fluorescence intensity remained constant. Fluorescence images at each pH were then captured (Figure 3a). As can be seen, the intensity of the para band remained nearly unchanged, while the ortho band showed higher intensity at more acidic pH values (see Figure S3a in Supporting Information for intensity line profile data). No evidence for hysteresis was observed by returning the pH back to 10.2 from 4.0 or even by cycling the pH several times. The normalized peak area of the ortho band relative to the para band as a function of pH is plotted in Figure 3b, and an apparent pK_A value of 7.8 ± 0.1 can be abstracted from the data.

Next, we attempted to determine how fast *ortho*-Texas Red DHPE can respond to bulk pH changes. To do this, two separated bilayer strips were formed containing the ortho and para dyes, respectively. Time-sequence fluorescence images were obtained as the bulk pH was abruptly increased from 4.0 to 10.2. The fluorescence micrographs and line profiles as a function of time are shown in Figure 4. As can be seen, the fluorescence changed almost as abruptly as the pH could be raised (i.e., within a few seconds). Such a result is in agreement with the response of an ortho-conjugated sulforhodamine isomer in bulk aqueous solution, which can respond to pH changes on the millisecond time scale.[26] Moreover, it appears that nearly all Texas Red DHPE molecules in the bilayer are rapidly able to sense the pH jump.

Titration Curve with a Saturated Protein Layer. The *ortho*-Texas Red DHPE isomer should be an excellent reporter for small changes in the local pH brought about by the binding of proteins from bulk solution. To demonstrate this principle the biotin/antibiotin antibody binding pair was employed as a test system. First, two separated bilayer strips were formed as described above. Then, the surface was saturated with antibiotin IgG by introduction of a 500 nM protein solution over the surface for 10 min. All subsequent measurements were made by tuning the solution pH but keeping the bulk IgG concentration constant.[36] The results shown in Figure 5 reveal an apparent shift of ~0.35 pH units with respect to the results in Figure 3,[37] which were taken in the absence of bound proteins.

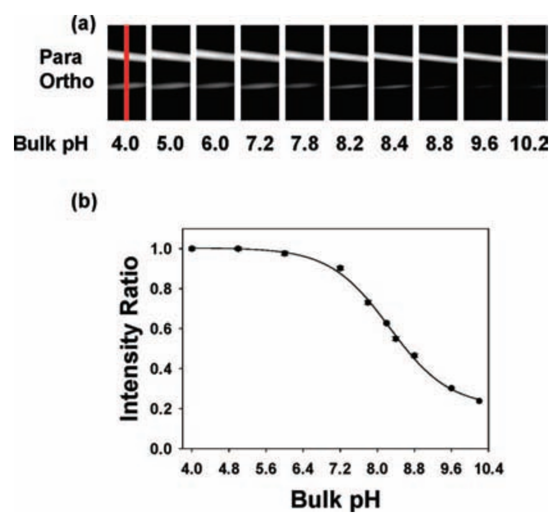

Figure 5. (a) Epifluorescence images of *para*-Texas Red DHPE (upper) and *ortho*-Texas Red DHPE (lower) strips at different bulk solution pH values in the presence of a saturation concentration of antibiotin. (b) Relative intensity ratio for *ortho*-Texas Red DHPE as a function of pH. The black circles represent fluorescence measurements, and the solid line is a sigmoidal fit to the data ($R^2 = 0.99$). To obtain the y axis, the intensity of the ortho band was divided by that of the para band at each pH value and the value at pH 4.0 was set to 1.0. All other intensity ratios are relative to this value. Error bars representing standard deviation measurements from three data sets are denoted on each data point. A 10× air objective was used to make these measurements. The red line across the first image in (a) denotes an example of the region from which intensity line profile data were abstracted. These data are provided in Figure S3 of the Supporting Information.

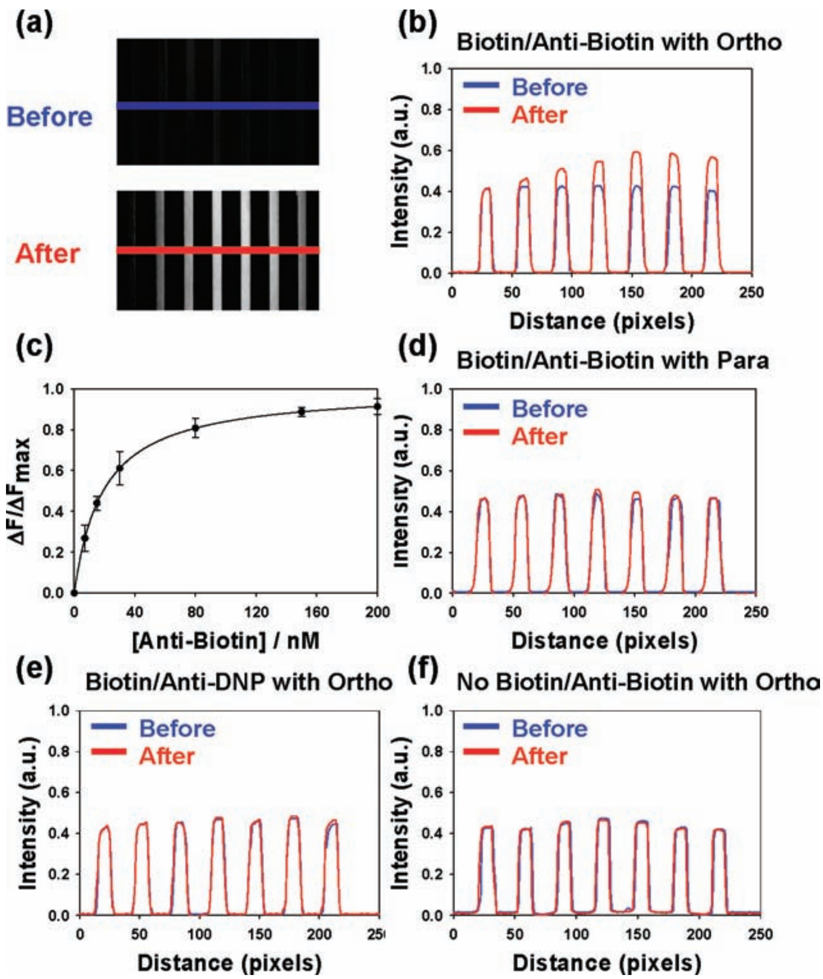

Figure 6. (a) Epifluorescence images of a bilayer-coated microfluidic device before and after introduction of unlabeled antibiotin antibodies. The concentration of the protein in the bulk solution was increased from left to right. The blue and red lines represent the regions used to obtain the line profiles shown in (b). (c) Plot of normalized fluorescence intensity ($\Delta F/\Delta F_{max}$) vs bulk protein concentration. The solid line represents the best fit to a Langmuir isotherm. (d) Experimental line profiles for the same conditions shown in (b) but with *para*-Texas Red DHPE in the membrane instead of the ortho form. (e) Experimental line profiles for the same conditions shown in (b) but with anti-DNP antibodies. (f) Experimental line profiles for the same conditions as in (b) but in the absence of biotin-cap-PE. A 4× air objective was used to make all measurements. It should be noted that each data point in (c) represents the average of three measurements and the error bars are standard deviations from those measurements.

Binding Curve for Antibiotin Antibodies. To obtain the equilibrium dissociation constant for the biotin/antibiotin system, POPC bilayers containing 0.5 mol % biotin-cap-PE and ~0.03 mol % *ortho*-Texas Red DHPE were coated on the inside walls and floors of a seven-channel PDMS/glass microfluidic device. Experiments were run in all channels at a bulk pH of 8.2. Concentrations of antibodies ranging from 0 to 200 nM were flowed continuously through the individual channels until the fluorescence intensity from the surface-bound dyes remained constant. Epifluorescence images from the device used in these experiments are shown in Figure 6a. As can be seen, weaker and uniform fluorescence intensity was observed in all channels before addition of protein. After the IgG molecules were introduced, the fluorescence intensity was strengthened in accordance with the bulk concentration of the antibodies.

Line profiles taken from the images (blue and red lines in Figure 6a) are plotted in Figure 6b. As can be seen, the fluorescence intensity after introduction of the protein molecules increased and then leveled off as the protein concentration was increased. It should be noted that the fluorescence intensity from the *ortho*-Texas Red DHPE was enhanced after protein binding by ~1.4 times at the highest two bulk protein concentrations. On the basis of the curve in Figure 3b, the initial fluorescence intensity was 42% of the maximum value and ended at 60% of the maximum value upon protein binding. It should be noted that this interfacial pH shift occurred in the regime where the fluorescence intensity varied nearly linearly with pH (Figure 3b).

The normalized increase in fluorescence intensity as a function of bulk antibody concentration from Figure 6b is plotted as a function of bulk protein concentration in Figure 6c. Specifically, the *y* axis plots the change in fluorescence intensity (ΔF) relative to the maximum change in fluorescence intensity when a saturation concentration of protein is present (ΔF_{max}).

(36) It should be noted that the IgG molecules did not noticeably aggregate as the pH was tuned between 4 and 10.2. In fact, no changes in the activity of antibiotin IgG were observed in the range of pH 4.0–10.2 (Supporting Information). This is to be expected as these proteins do not possess a single isoelectric point (pI) as the population is polyclonal.

(37) The apparent shift of ~0.35 pH units corresponds to the shift in the midpoint of the titration curve for Figure 5b with respect to Figure 3b as determined by a sigmoidal fit to the data.

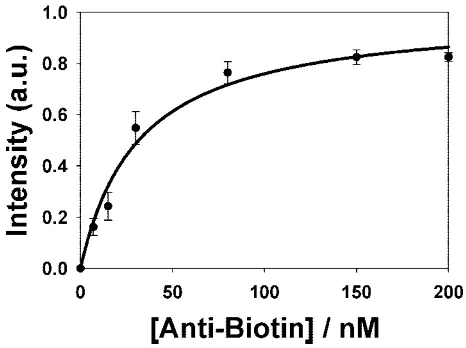

Figure 7. Plot of TIRFM intensity vs bulk protein concentration for the labeled antibiotin/biotin binding system. Each data point represents the average of three measurements, and the error bars are standard deviations from those measurements. The solid curve through the data is the best fit to a Langmuir isotherm.

In order to extract the apparent equilibrium dissociation constant (K_D) the biotin/antibiotin binding curves were fit to a simple Langmuir isotherm binding model (eq 1):

$$\Delta F = \Delta F_{\max}\frac{[P]}{K_D + [P]} \tag{1}$$

where $[P]$ is the bulk antibody concentration. The fit to the curve for the data in Figure 6c yields $K_D = 24 \pm 5$ nM.

The biotin/antibiotin binding experiments were repeated under a nearly identical set of conditions but using *para*-Texas Red DHPE instead of the ortho form. The fluorescence line profiles both before and after antibody binding are shown in Figure 6d. As can be seen, little if any change in fluorescence intensity occurred under these conditions. Several additional control experiments were also performed. For example, anti-DNP antibodies, which are not specific for biotin, were used instead of the antibiotin antibodies. Also, experiments were performed with antibiotin antibodies and *ortho*-Texas Red DHPE but without any biotin-cap-PE in the membrane. In both of these cases the fluorescence intensities from the microchannels remained unchanged within experimental error upon introduction of protein (Figure 6e and 6f, respectively). Such results are consistent with both high ligand−receptor specificity as well as relatively low levels of nonspecific protein adsorption to the surface.

Next, classical antibody binding experiments were performed using antibiotin antibodies labeled with Alexa Fluor-594 dye (Figure 7). Binding measurements were made by total internal reflection fluorescence microscopy (TIRFM)[38] as described previously.[34] In this case the supported membranes contained 99.5 mol % POPC and 0.5 mol % biotin-cap-PE. These experiments yielded a K_D value of 32 ± 7 nM. Therefore, the classical label and pH modulation assays gave nearly identical results within experimental error. Moreover, both values correlated well with previously reported values for biotin/antibiotin interactions on supported membranes.[39]

The similarities between the classical and pH modulation measurements as well as the associated control experiments are strong evidence for the reliability of the new assay. Specifically, the change of fluorescence intensity in the pH modulation assay appears to correlate linearly with the interfacial antibody concentration under the conditions of these measurements. Moreover, it should be noted that this assay is far easier to perform than its protein-labeled counterpart. In fact, the classical binding assay requires that the antibodies be conjugated with fluorescent dye molecules and that free dye be subsequently separated from the labeled antibodies by running the mixture down a size exclusion column. Once the labeled antibodies are introduced into the microchannels the fluorescence assay must discriminate between antibodies bound to the surface and those in the bulk solution above it. As noted above, this was done in the present case by TIRFM, a surface-specific technique that requires a laser beam to be introduced to the sample past the angle of total internal refection.[35] By contrast, the pH modulation assay can be run in standard epifluorescence mode because the pH-sensitive dye molecules are already located at the interface within the supported bilayer. Of course, no modification of the antibodies is needed to do these experiments.

Limit of Detection (LOD) Measurements. In a final set of experiments we wished to determine the LOD value for this pH sensor assay by two different metrics. First, the CCD camera was used in imaging mode to determine the fewest number of IgG molecules that could be sensed. In that case 4×4 pixel binning was employed, which corresponds to a 1.7 μm^2 area at the lipid bilayer interface. Second, the experiments were repeated with 200×200 pixel binning to determine the lowest number density of IgG molecules which could be detected. The camera contains a 1024×1024 pixel array.

To perform 4×4 binning experiments, supported bilayers were made from POPC lipids doped with 0.5 mol % biotin-cap-PE and ~0.03 mol % *ortho*-Texas Red DHPE. Concentrations of antibiotin IgG ranging from 0 to 100 pM were introduced into the bulk solution. Line profiles both before and after introduction of the protein are shown in Figure 8. As can be seen, the fluorescence intensity remained essentially unchanged when 0 pM antibiotin was added (pure PBS buffer flowed for 60 min), but changed by ~8% when 100 pM antibiotin was added. It should be noted that intensity changes were linear with concentration between 0 and 100 pM antibody as shown in Figure 8f (red circles). The slope of the line and its corresponding R^2 value are provided as an inset in the figure.

Error analysis of the intensity profiles revealed that the averaged fluorescence intensity over a given channel was stable to within ±0.2% over a 1 h time period. This gives an LOD value of ~8 pM if the limit of detection is defined as 2.58 times the experimental error. It should be noted that this definition of LOD was chosen because it represents the 99% confidence limit for these measurements.[40] Control experiments with *para*-Texas Red DHPE under the same conditions showed that little if any change in fluorescence intensity occurred when the antibody was introduced (Figure 8f, black circles). Additional control experiments were performed with anti-DNP as well as without any biotin-cap-PE in the membrane (data not shown). No observable change in fluorescence intensity occurred.

Next, the LOD was determined using 200×200 pixel binning. This dimension, which represents a 65 μm × 65 μm region of the liquid/solid interface, was chosen because it corresponds well to the width of an individual microfluidic channel. The experimental conditions were identical to those used above. Concentrations of antibiotin ranging from 0 to 1.5 pM were introduced into the bulk solution. In this case, single

(38) Axelrod, D.; Burghardt, T. P.; Thompson, N. L. *Annu. Rev. Biophys. Bioeng.* **1984**, *13*, 247–268.
(39) Blake, R. C.; Pavlov, A. R.; Blake, D. A. *Anal. Biochem.* **1999**, *272*, 123–134.
(40) Christian, G. D. *Analytical Chemistry*, 6th ed.; John Wiley & Sons, Inc.: New York, 2004.

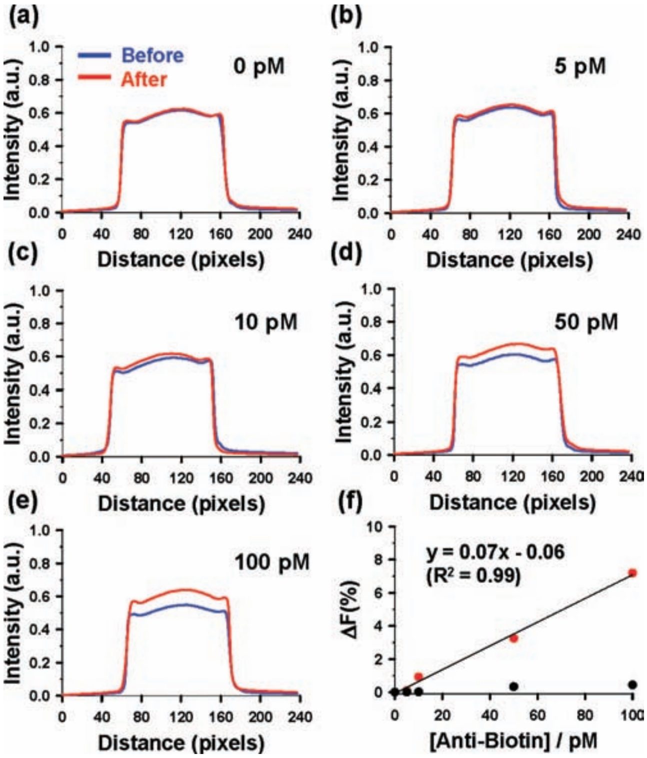

Figure 8. LOD results for 4 × 4 pixel binning. (a–e) Intensity line profiles across single microfluidic channels as various concentrations of antibiotin antibodies were introduced to the bulk solution. The experiments were conducted at a bulk pH of 7.8 in 10 mM PBS with 150 mM NaCl. (f) Plot of the change in the fluorescence intensity of *ortho*-Texas Red DHPE, ΔF (%), vs bulk protein concentration (red circles). The slope of the line and its corresponding R^2 value are provided in the figure. A control experiment was also performed with *para*-Texas Red DHPE in the membrane under otherwise identical conditions (black circles).

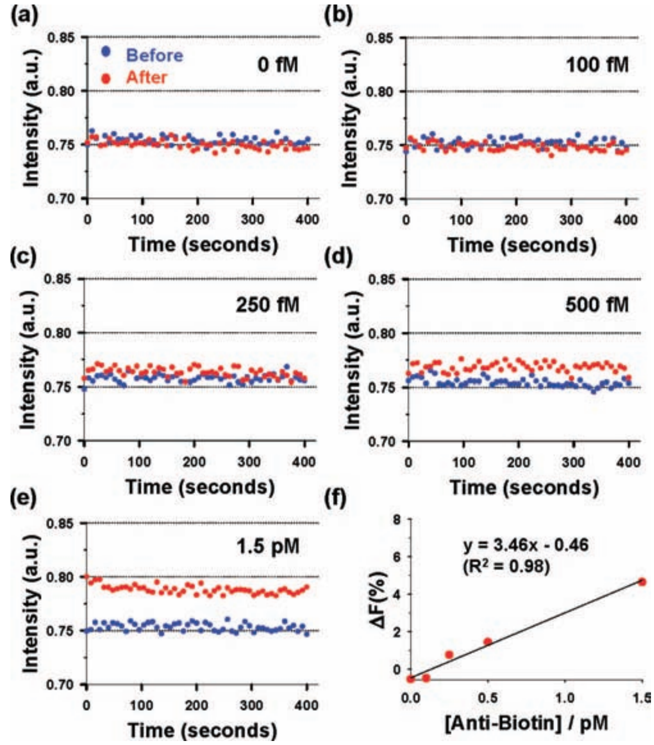

Figure 9. LOD results for 200 × 200 binned pixel regions. (a–e) Single-point fluorescent intensity measurements as a function of time both before and after introduction of various concentrations of antibiotin. (f) Plot of fluorescence intensity for *ortho*-Texas Red DHPE, ΔF (%), vs bulk protein concentration (red circles). The slope of the line and its corresponding R^2 value are provided in the figure.

data point intensities were recorded as a function of time (Figure 9a–e). Approximately 50 data points were obtained for each sample region over the course of 400 s both before and after introduction of protein. This was done to further improve the signal-to-noise of the experiment. As can be seen, the fluorescence intensity remained stable to within ±0.3%. The data at each antibody concentration were averaged and plotted in Figure 9f (red circles). The LOD value was found to be ~350 fM at the 99% confidence limit.

Discussion

We developed a novel pH-sensitive assay for monitoring ligand/receptor binding at lipid membrane interfaces. The method should be quite general since most biomacromolecules in solution bear a net charge. Specifically, we found that a shift of ~0.35 pH units occurred upon saturation binding of IgG to a lipid membrane with 0.5 mol % lipid-conjugated haptens compared to the case of no bound proteins. Such a result is in agreement with the notion that increasing the density of negative charge at the interface recruits counterions (especially hydronium ions). In fact, Fromherz suggested that changes in membrane potential can affect the interfacial concentration of hydronium ions and thereby shift the local pH.[41] Also, Latour and co-workers demonstrated that deprotonated COOH-terminated self-assembled monolayers (SAMs) attract hydronium ions to the interface, thus resulting in a decrease of the local pH value.[42] Changes in interfacial charge density, therefore, should lead to corresponding shifts in the apparent pK_A values of titratable surface groups relative to their values in bulk solution.[24] This makes the titration of fluorescent dye molecules useful for sensor development. How useful this phenomenon can be for assay development ultimately depends upon its sensitivity.

Sensitivity limits for biosensor platforms are often reported in the literature in terms of the minimum bulk analyte concentration that can be detected.[43] However, the LOD is usually strongly correlated to the strength of a given ligand/receptor binding event. For example, a typical antibody/antigen interaction might have a K_D value of 25 nM, while a tighter protein/ligand interaction could be $K_D \approx 1$ pM. A heterogeneous detection assay (i.e., detection of the analyte by binding to a surface from solution) might have a detection limit of 250 pM for the former but 10 fM for the latter. In reality, these apparently different bulk detection limit values may actually represent similar number densities of proteins at the interface because each LOD value would be 1% of K_D. Therefore, the number of proteins at the interface which can be detected may represent a more intrinsic measure of the LOD value for a particular assay platform.

In the studies described in Figure 8 we employed 0.5 mol % biotin-cap-PE and used 4 × 4 pixel binning of our CCD camera with a 40× oil immersion objective for detection. This corre-

(41) Fromherz, P. *Methods Enzymol.* **1989**, *171*, 376–387.

(42) Fears, K. P.; Creager, S. E.; Latour, R. A. *Langmuir* **2008**, *24*, 837–843.

(43) Liang, M.; Klakamp, S. L.; Funelas, C.; Lu, H.; Lam, B.; Herl, C.; Umble, A.; Drake, A. W.; Pak, M.; Ageyeva, N.; Pasumarthi, R.; Roskos, L. K. *Assay Drug Dev. Technol.* **2007**, *5*, 655–662.

sponds to a 1.7 μm^2 surface area at the liquid/solid interface for each binned pixel region. The area per lipid molecule in the membrane is known to be $\sim$0.7 nm^2/lipid.[44] By assuming that biotin-cap-PE is roughly the same size as the lipids, 0.5 mol % of this molecule translates to $\sim 7 \times 10^3$ ligands/μm^2 on the upper bilayer leaflet. The intensity change at 500 nM IgG is $\sim$150 times greater than that observed at the LOD ($\sim$8 pM). Therefore, the number density of proteins at the interface should be $\sim$150 times less than the saturated value. This results in a detection limit of $\sim$380 IgG molecules if one assumes a 2:1 binding ratio between the antibody and the antigen.[35] Such a nonoptimized result is within a few orders of magnitude of single molecule measurements. This result corresponds to a surface density of 56 pg/mm^2. This surface density LOD value can be substantially improved by binning together a larger number of pixels while making the binding measurements. Although one loses the ability to obtain a surface image, the signal-to-noise ratio should roughly improve with the square root of the number of pixels employed. Additional improvements can be obtained by time averaging. The data for 200 $\times$ 200 pixel binning are provided in Figure 9. Such data represents an antibody surface density of $\sim$2 pg/mm^2. Moreover, the 350 fM LOD is a factor of $\sim$69 000 lower than the K_D value of 24 nM, although one is no longer sensing just a few hundred IgG molecules. It should be possible to sense even lower number densities of proteins by binning an even larger number of pixels together. Indeed, simultaneous sensing over a 1 mm^2 area should reduce the number density detection limit by yet another order of magnitude. In that case, however, the ability to perform multiplex detection is completely eliminated.

Currently, surface plasmon resonance (SPR) is one of the most commonly employed label-free assays for monitoring ligand/protein binding at an interface. Direct comparisons between assays can sometimes be problematic. Therefore, we will limit this discussion to antibody/antigen binding measurements. In that case, SPR platforms in a Kretschmann configuration[45] gave rise to an LOD of $\sim$3 pM for a system with a K_D value of $\sim$4 nM.[14] For the present assay, we achieved a detection limit significantly better than that ($\sim$350 fM out of 24 nM). Of course, the sensitivity limits for SPR and SPRI can be vastly improved by secondary amplification steps.[6,46,47] By analogy, LOD from the current pH modulation assay could also be substantially enhanced by subsequent amplification procedures after antibody binding.

It should be noted that the pH modulation platform developed here should be highly versatile. Binding measurements were made on two dimensionally fluid lipid bilayers because these systems are laterally mobile and should allow the same type of multivalent protein binding to take place as occurs in vivo on a cell surface.[48] Moreover, supported lipid bilayer platforms are highly resistant to nonspecific protein adsorption.[49] Nevertheless, this sensing concept could be expanded to any liquid/solid interface that contains substrate-conjugated ligands and pH-sensitive fluorophores. It should also be capable of measuring nearly any protein−ligand binding event provided that the incoming macromolecule possesses a net charge and therefore changes the interfacial pH. As another demonstration of the universality of this method, the binding of cholera toxin B to ganglioside GM_1 is provided in the Supporting Information section (Figure S5).

In conclusion, a simple detection method based on pH-sensitive dyes was developed. Specifically, ortho-conjugated Texas Red DHPE incorporated in supported phospholipid bilayers was used as an interfacial pH sensor. Such sensors have inherently excellent limits of detection and are relatively easy to use. Moreover, the method is fully compatible with multiplexed detection. Therefore, it could potentially be used in high-throughput screening applications.

Acknowledgment. We thank the Office of Naval Research (N00014-08-1-0467), the NIH (R01 GM070622), and the ARO (W911NF-05-1-0494) for support. We also thank Dr. Jinjun Shi and Dr. Tinglu Yang for technical assistance, Dr. Xin Chen for critical comments on the manuscript; and Jun Yong Kang for help with bulk dye separation.

Supporting Information Available: Experiments concerning the bilayer quality and stability at various pH values, quantitative fluorescence line scan data for Figures 3a and 5a, as well as binding data for cholera toxin B to GM_1. This material is available free of charge via the Internet at http://pubs.acs.org.

JA804542P

(44) White, S. H.; King, G. I. *Proc. Natl. Acad. Sci. U.S.A.* **1985**, *82*, 6532–6536.
(45) Kretschmann, E. *Z. Phys.* **1971**, *241*, 313–324.
(46) Fang, S. P.; Lee, H. J.; Wark, A. W.; Corn, R. M. *J. Am. Chem. Soc.* **2006**, *128*, 14044–14046.
(47) Goodrich, T. T.; Lee, H. J.; Corn, R. M. *J. Am. Chem. Soc.* **2004**, *126*, 4086–4087.
(48) Kim, J.; Kim, G.; Cremer, P. S. *Langmuir* **2001**, *17*, 7255–7260.
(49) Castellana, E. T.; Cremer, P. S. *Surf. Sci. Rep.* **2006**, *61*, 429–444.